On-Line Visualization of Dye Diffusion in Fresh Unfixed Human Skin

Ylva Y. Grams,[1] Lynne Whitehead,[2] Paul Cornwell,[2] and Joke A. Bouwstra[1,3]

Received October 2, 2003; accepted February 5, 2004

Purpose. The purpose of the current study was to develop a new method to examine the diffusion in fresh unfixed human skin on-line.
Methods. Full thickness skin samples were cut perpendicular to the skin surface (cutting plane facing upwards) with a new cutting device forming part of the final diffusion cell. The donor solution contained 0.1 mg/ml Bodipy FL C_5 (moderately lipophilic) dissolved in citric acid buffer, pH 5.0, and the acceptor phase consisted of phosphate-buffered saline, pH 7.4. Images were taken with confocal laser scanning microscopy (CLSM) every 10 min for 8 h.
Results. This new method enabled for the first time visualization of concentration profiles in different skin layers simultaneously as a function of time. For this model penetrant, Bodipy FL C_5 showed that the lower stratum corneum layer constitutes the greatest barrier to diffusion. Furthermore, there is preferred partitioning of this probe in epidermis vs. either stratum corneum or dermis.
Conclusions. The on-line diffusion cell in combination with CLSM is a promising tool to study diffusion processes of dyes in fresh unfixed skin on-line. The method has the potential to access deeper skin layers as well as to visualize diffusion processes in cells.

KEY WORDS: confocal laser scanning microscopy; depth-resolved; on-line visualization; time-resolved; unfixed full-thickness human skin.

INTRODUCTION

In pharmaceutical and cosmetic research, the distribution of penetrating probes is of great interest for understanding and improving drug efficacy. This distribution is accessible by visualization of the skin, focusing either on the stratum corneum, the epidermis, or on deeper layers of the skin including its appendages. The latter is especially of interest for local delivery to the sweat glands or to the pilosebaceous unit (sebaceous gland and the hair follicle).

Recently, techniques used so far in skin imaging (1) or in quantification of substance distribution within the skin have been reviewed elsewhere (2). In summary, local targeting of a drug and its distribution in the skin can be investigated using i) only one time-point or ii) multiple time-points or even continuous visualization in one piece of skin. In the first case, visualization methods including postexperimental processing like fixation or staining are feasible (1,2). However, they bear the danger of artefact formation or delocalization of the label. In the second case, postexperimental processing of the skin (cutting or chemical fixation) is not acceptable, as it would influence the diffusion process of the substance. Additionally, minimization of the variation between time points by using skin of the same donor is an advantage.

In literature, various techniques have been described that are feasible for real-time visualization of skin, namely video fluorescence imaging (3), video microscopy (4–7), magnetic resonance imaging (8–10), electron paramagnetic resonance (11), ultrasound backscatter microscopy (12), Raman spectroscopy (13,14), and various modifications of confocal microscopy (15–21). Though techniques like fluorescence imaging, magnetic resonance imaging, and ultrasound backscatter microscopy have a limited resolution; techniques like fluorescence imaging and video microscopy are limited to the visualization of the upper layers. Confocal microscopy and confocal Raman spectroscopy can access deeper layers such as the upper dermis due to optical sectioning even *in vivo*.

In our studies, confocal laser scanning microscopy (CLSM) in combination with fluorophores has been used. This has the advantage that the skin can be visualized without fixation and that the resolution is sufficient to visualize the various layers of the hair follicle. However, the deeper layers of the dermis are not accessible due to scattering and absorption processes of the fluorescence signal. For this reason, a method has been developed in our group limiting the artefact formation by cross-sectioning *fresh* human skin (22). More recently, this technique was extended to full-thickness skin (23). This method allows examining the distribution of fluorophores in the various skin compartments after a predetermined period of diffusion. Although this provides detailed information on the fluorophore accumulation in the various skin compartments, it is not possible to gain information on the permeation pathways of the active agents. For information on permeation pathways, on-line visualization of diffusion processes is required. Therefore, the aim of our current study is to develop a visualization method enabling real-time image acquisition in the same donor using human skin. Because future studies will be focused on target areas in deeper skin layers such as the pilosebaceous unit, the subcutaneous tissue is also included.

MATERIALS AND METHODS

Model Substance

Two fluorophores were selected to develop the diffusion cell used for on-line CLSM visualization, subsequently named "on-line diffusion cell." Oregon Green 488, a low-molecular-weight molecule with a $\log P_{octanol/buffer}$ of 1.6 at pH 5.0 and –2.5 at pH 7.4, was selected for leakage tests due to poor penetration in the skin. Bodipy FL C_5, a low-molecular-weight compound with a $\log P_{octanol/buffer}$ of 2.5 at pH 5.0 and 1.2 at pH 7.4, was used for the on-line experiments due to its good staining properties. Both fluorophores were purchased from Molecular Probes (Leiden, The Netherlands). Impregum F was obtained from Espe (Seefeld, Germany) and the pioloform from Agar Scientific Ltd. (Stansted, UK).

Confocal Laser Scanning Microscopy

The visualization of the fluorophores in the *non-fixed* scalp skin (three donors) was carried out using a Bio-Rad

[1] Leiden/Amsterdam Center for Drug Research, Department of Pharmaceutical Technology, Leiden University, 2300 RA Leiden, The Netherlands.
[2] Unilever Research, Port Sunlight, UK.
[3] To whom correspondence should be addressed (e-mail: bouwstra@lacdr.leidenuniv.nl)

0724-8741/04/0500-0851/0 © 2004 Plenum Publishing Corporation

MRC 600 U equipped with an Argon laser with an emission line at 488 nm (Veenendaal, The Netherlands). The microscopic unit consisted of an inverted Zeiss IM-35 using a PlanApo 20 or PlanApo 63 oil immersion objective (Jena, Germany). The cross-sectional view of the skin is obtained by using a modified cutting device according to Meuwissen *et al.* (22), which is used as a sample holder at the same time.

Donor and Acceptor Phase

The donor solutions contained 0.1 mg/ml Oregon Green 488 or 0.1 mg/ml Bodipy FL C_5in citric acid buffer, pH 5.0. The donor compartment was completely filled with the donor solution, which was approximately 100 μl, with slight variations due to the dental clay usage. Care was taken to circumvent air enclosure in the donor compartment. The acceptor phase consisted of phosphate buffered saline pH 7.4 (139 mM NaCl, 2.5 mM KCl, 8 mM Na_2HPO_4, 1.5 mM KH_2PO_4, 25 mg/L streptomycin, and 25000 U/l penicillin). The acceptor compartment was a static compartment of approximately 100 μl with small variations in size due to the dental clay sealing.

Preparation of On-Line Diffusion Cell

The design and the preparation procedure of the on-line diffusion cell are depicted in Fig. 1. Briefly, the stratum corneum surface of a fresh human scalp skin square (8 × 8 mm) including the subcutaneous fat is wiped with PBS and 70% (v/v) ethanol to remove any contaminants and placed in the equivalent space of the cutting device (Fig. 1, II). A silicone square with a pre-cut smaller square (4 × 2.5 mm) is supporting the skin at the stratum corneum side thereby preventing artefact formation during the cutting procedure (Fig. 1, II). After cutting perpendicular to the skin surface, only one half of the cutting device is used (Fig. 1, III). The smaller square is removed carefully, and a drying protection is placed above the cutting surface not touching the skin (not shown). Mounting the donor compartment to the cell completes the assembly (Fig. 1, IV). A thin layer of dental clay (Impregum F) surrounds the skin and the cell compartments in the cutting plane (not shown). A pioloform-coated cover glass [0.5% (w/v) pioloform in chloroform, not shown] is placed on top of the dental clay and the skin, thereby sealing the on-line diffusion cell. After complete hardening of the dental clay, the acceptor phase is injected through the dental clay, and the pioloform is removed from the accessible side of the cover glass with 70% (v/v) ethanol. The on-line cell is now placed in a holder and subsequently in an adapter for the microscope (Fig. 1, V–VI).

Image Acquisition

The cross section is localized using its low autofluorescence with sensitive CLSM settings. Images were collected every 10 min starting 10 min after application of the donor phase for a period of 8.5 h. Obvious leaking on-line preparations were immediately discarded from investigation. When the swelling appeared to have a severe influence on the movement of the point of focus, the results were discarded as well. During the experiment, the temperature of the skin is not monitored. All measurements have been carried out at room temperature.

Test for Leakage

In a pilot experiment, the on-line diffusion cell was checked for leakage between the cover glass and the skin. For this purpose, skin from the same donor was visualized after a 2-h application in a flow-through diffusion cell from PermeGear (Bethlehem, USA) and for 2 h in an on-line diffusion cell.

Image Analysis

In the image analysis of the on-line series, it has to be assumed that the fluorescence of one molecule is independent of the skin part. Therefore, a model drug has been chosen that is reported to be insensitive to pH and solvent polarity (24). Although the measurement of the fluorescence results in a two-dimensional image, the actual focal plane is three-dimensional. Therefore, the obtained fluorescence is the integrated fluorescence from a constant volume around the focal plane. The images of the time series were analyzed using Image J software. A gray scale displays fluorescence intensities in one image with 0 (black) as the minimal and 254 (white) as the maximal value. In order to obtain an average value for the fluorescence intensity of a pixel in depth, a box of 50 pixels wide and a length determined by the cross section (>300 pixels) was chosen and placed across the image perpendicular to the stratum corneum The analyzed box is displayed above each distribution profile. The change of fluorescence in time (dF/dt) and in depth from the skin surface (dF/dx) was recorded. The stratum corneum was divided into three layers (top, middle, and deep) and the viable epidermis in two layers (top, deep) while only the upper layers of the dermis could be analyzed.

Fick's law describes that the transported mass dm (g) per time unit dt (h) through a defined area A (cm^2) is directly proportional to the diffusion coefficient D (cm^2/s), the size of the area and the concentration change dc (g/cm^3). However it is reverse proportional to the thickness of the membrane dx (cm).

$$\frac{dm}{dt} = -DA\frac{dc}{dx} \tag{1}$$

The change of concentration with depth (dc/dx) in a defined time period is proportional to the change of fluorescence in depth (dF/dx) in the same time period. The proportionality is unknown in CLSM however can be expressed by introducing a proportionality factor K_c.

$$\frac{dc}{dx} = K_c\frac{dF}{dx} \tag{2}$$

In a steady-state situation, the mass transported across the stratum corneum, the viable epidermis, and the dermis are equal, as no accumulation in each of the skin layers occurs. Therefore, a relation between the diffusion coefficients of the various skin layers can be estimated, and consequently, the influence of different skin layers on the diffusion of a dye through the skin can be compared. However it has to be realized that using Fick's law of diffusion is an approximation

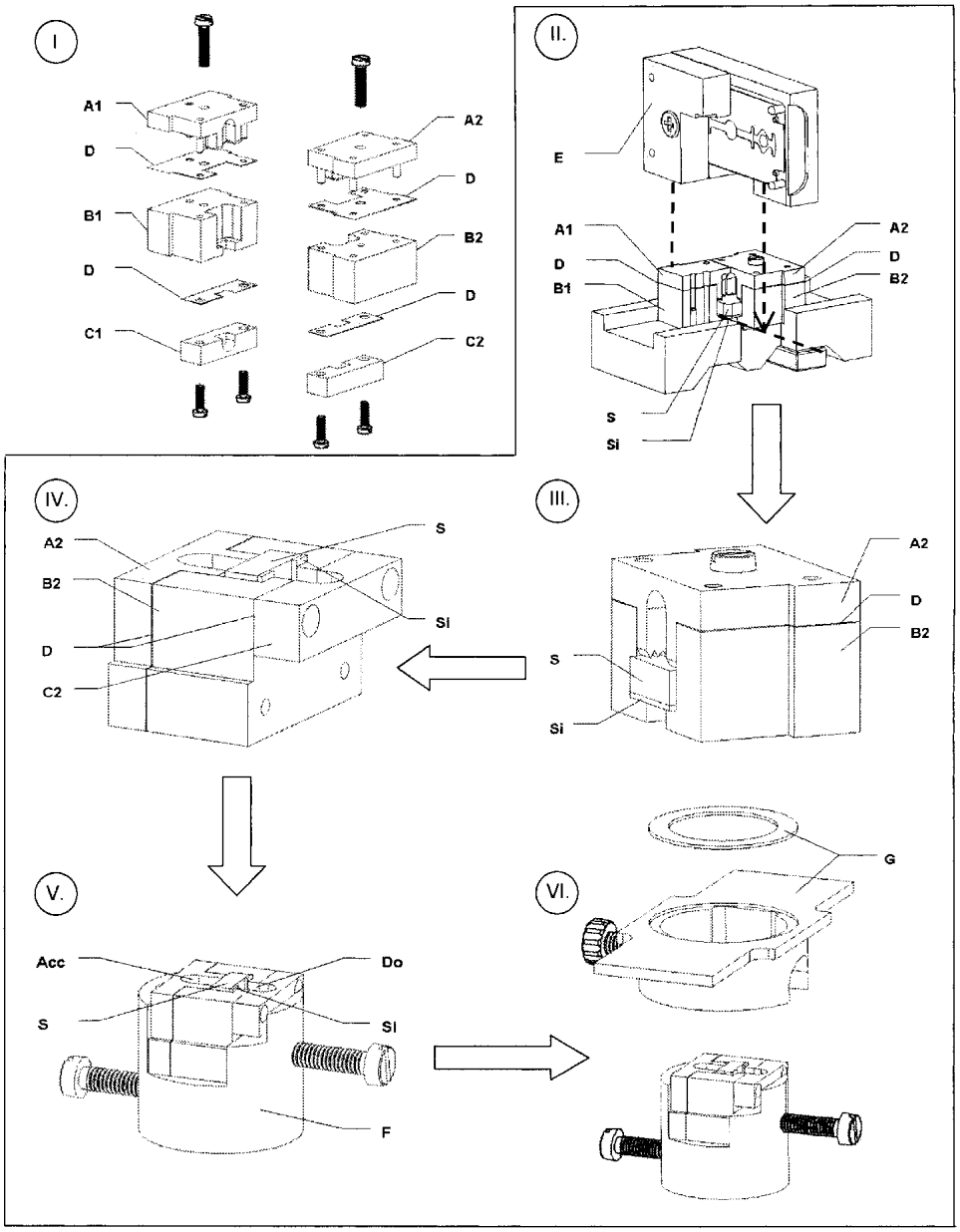

Fig. 1. Composition and preparation of the on-line diffusion cell with A, acceptor phase compartment; B, skin compartment; C, donor phase compartment; D, teflon sheet; E, cutting knife containing razor blade; S, skin; Si, silicone square; Acc, acceptor phase; Do, donor phase; F, diffusion cell holder; G, microscope adapter. "I" shows the combined cutting and visualization device, whereas II–VI depicts the preparation process of the on-line diffusion cell. A piece of skin including the subcutaneous fat is placed in the equivalent compartment of the cutting device with the stratum corneum side facing down (II). After cutting perpendicular to the skin surface (II), one half of the cutting device will be used for further processing (III). The donor compartment (C2) will be attached to the cutting device resulting in a cross-sectional view of the skin with the adjacent donor and acceptor compartment (IV). The cross section is sealed with cover glass and dental clay (not shown) and subsequently placed in diffusion cell holders to enable visualization in the CLSM (V and VI).

in our experimental setup as the donor and acceptor phase were both static.

RESULTS

Test for Leakage

To ensure that the observed diffusion is not due to leakage of label between the cutting surface and the cover glass, the setup was checked for leakage. Neither a preliminary test with a methylene blue solution (not shown) nor the comparison of 2 h penetration of a hydrophilic Oregon Green 488 in skin of the same donor using the static (Fig. 2, IA) and the on-line mode (Fig. 2, IB) revealed any indication of leakage. With identical microscopic settings, comparable images were obtained. In both cases neither the epidermis nor the dermis revealed significant staining.

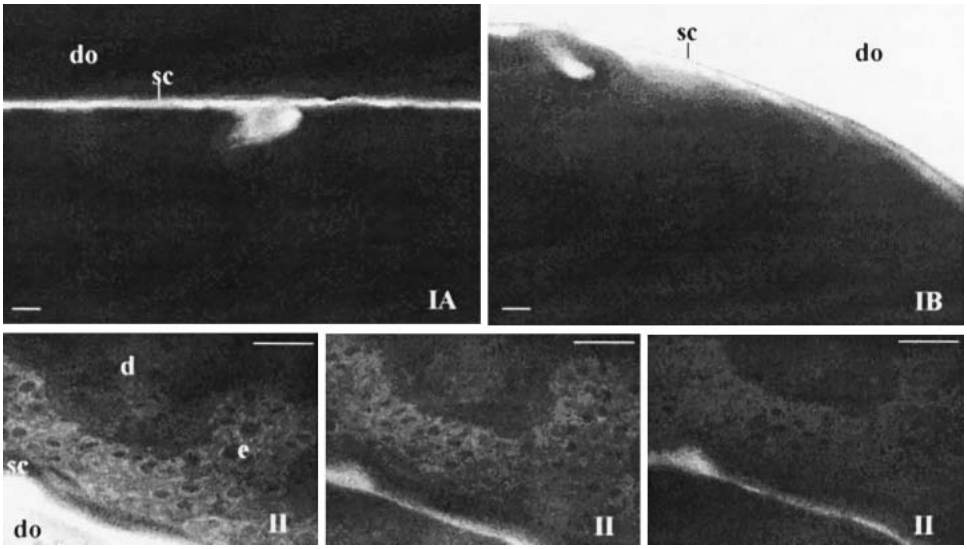

Fig. 2. Tests for leakage of the on-line diffusion cell. IA shows the distribution of 0.1 mg/ml Oregon Green 488 in citric acid buffer pH 5.0 after 2 h application in a PermeGear flow-through diffusion cell after postexperimental cross sectioning. IB is the view of the skin cross-section in the on-line diffusion cell after 2 h application of the same donor solution. The donor solution is still present in the on-line diffusion cell. No indication of leakage is present. Do, donor phase compartment; sc, stratum corneum. Images II show the distribution of 0.1 mg/ml Bodipy FL C_5 in citric acid buffer, pH 5.0, in the on-line diffusion cell after 10 min (IIA), 4 h 10 min (IIB), and 8 h 20 min (IIC). This time series is a positive example of leakage. If leakage was observed, the on-line preparation was discarded immediately. d, dermis; e, epidermis. The scale bar represents 25 μm.

On-line experiments were started using Bodipy FL C_5. Fig. 2, IIA–IIC, depict one skin preparation where leakage of the Bodipy FL C_5 along the cover glass is obvious. The images reveal an immediate presence of label in the epidermal layer. Furthermore, no increase in label intensity could be observed. A decrease in fluorescence intensity up to the end of image acquisition took place. In on-line experiments where leakage was suspected as in Fig. 2, IIA–IIC, the prepared skin was discarded.

On-Line Diffusion

With the on-line diffusion cell and the described method of preparation, it is possible to examine the diffusion of a fluorophore in unfixed fresh human skin from the stratum corneum across the viable epidermis into the dermis (Fig. 3). Shortly after the application of the donor solution, only the donor phase and the skin interface can be distinguished. In the diffusion process, the stratum corneum is labeled first, with strong labeling at the surface, followed by the epidermis and the dermis. At late time points, the staining of the epidermis is stronger than in the lower part of the stratum corneum and the dermis. Additionally, details of the epidermis such as the cell nuclei can be monitored as well.

Distribution Profile in Time

Due to the Image J analysis of the time series, a distribution profile of the fluorescence in a 10-min time-interval at pixel resolution is obtained (Figs. 4 and 5). The distribution profiles in time vary between the three donors (Fig. 5). Differences are observed in thickness of the stratum corneum and the viable epidermis as well as in the average fluorescence intensity values (maximum values in the raw data range from 110 for donor 1 up to >254 for donor 3). However gradients within one skin layer and relative fluorescence differences between the layers are comparable between the various donors. Focusing at the profile itself, at early time points, label is detected only in the stratum corneum where the intensity increases fast with time. After 8 h it appears that within the stratum corneum, the fluorescence gradient in depth is dependent on the position and not constant throughout the stratum corneum. The region close to the surface is characterized by a steep fluorescence gradient in the stratum corneum, whereas a less steep fluorescence gradient is observed in the stratum corneum region close to the viable epidermis. In the viable epidermis, low fluorescence intensity is observed at early time points and increases with time. At late time points, an abrupt increase in fluorescence intensity is observed for donor 1 and 2 at the junction between the stratum corneum and the viable epidermis. At the same time, a significant decrease ($p < 0.001$) in fluorescence intensity in the second half of the epidermis is observed for all three donors up to the epidermal-dermal junction. Local fluctuations in the profile of the epidermis correspond to smaller structures such as nuclei as seen in the analyzed box (Fig. 4). At the junction of viable epidermis and dermis, the intensity drops significantly for all three donors. The dermis reveals in all three donors a constant increase in fluorescence intensity in time until a maximum is reached. However, nothing can be said about the distribution within the dermis because due to the microscopic settings, only the first few micrometers are accessible in these time series. Although no differences between the stratum corneum and the viable epidermis at late time points were observed for donor 3 due to saturation of the signal, at early time points similar profiles were observed as with donors 1 and 2. Regarding the difference between the

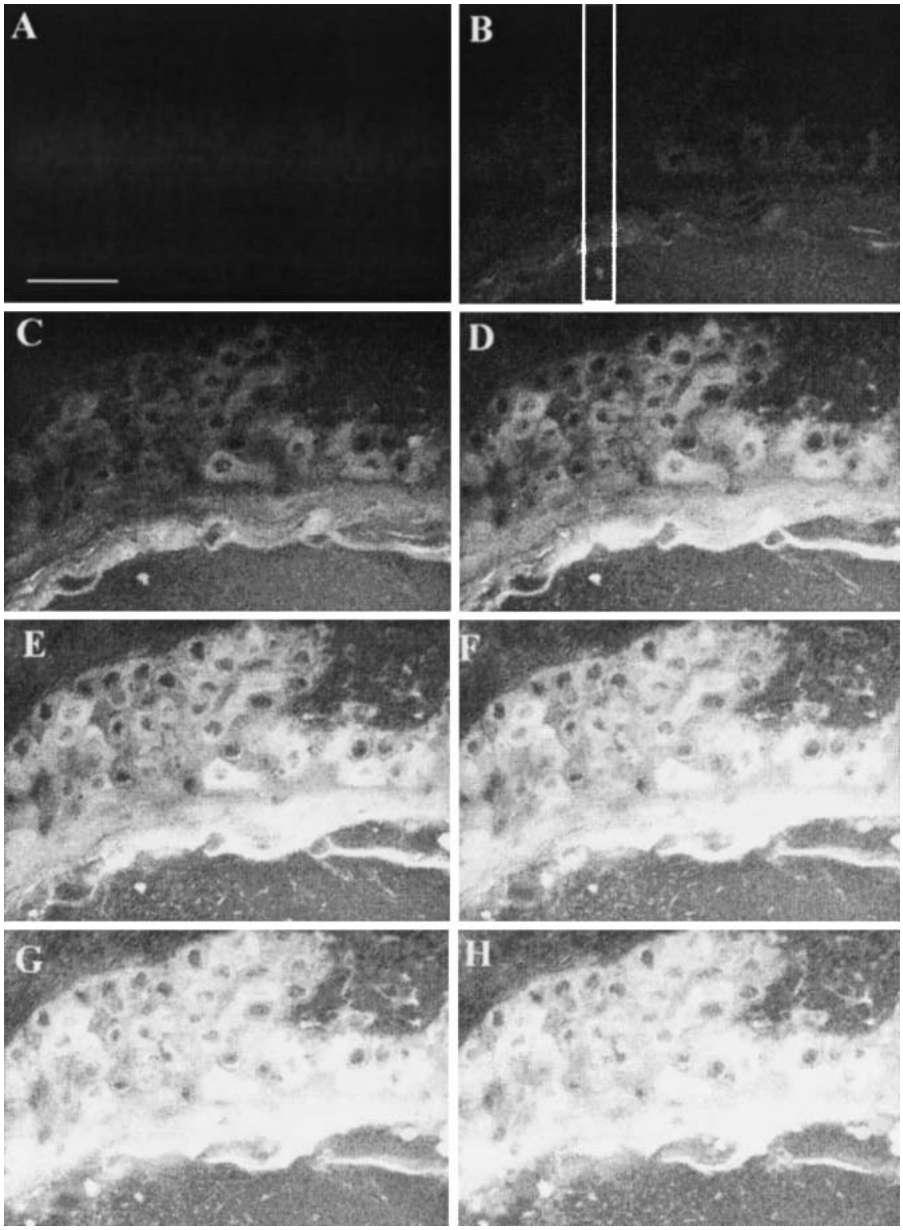

Fig. 3. A typical example of on-line visualization of the distribution of 0.1 mg/ml Bodipy FL C_5 in citric acid buffer applied at time point 0 in the donor compartment. Images were obtained every 10 min from which time points 10 min (A), 50 min (B), 1 h 30 min (C), 2 h 10 min (D), 2 h 50 min (E), 3 h 30 min (F), 4 h 10 min (G), and 4 h 50 min (H) are displayed. The box depicted in B resembles the quantified area at all time points that are provided in Fig. 5. The scale bar is equivalent to 25 μm.

viable epidermis and the dermis at late time points, this observation is also in agreement with donor 1 and donor 2.

Figure 6 displays the fluorescence gradient in depth of the various skin layers. Values of different donors were treated separately due to variations in the detected fluorescence signal despite the same settings of the microscope for all the on-line experiments. The stratum corneum reveals the highest fluorescence gradients; however, the gradients decrease with depth. In the viable epidermis, rather low gradients are observed, which increase in the lower half of the viable epidermis. The dermis reveals hardly any fluorescence gradient in the visualized layers. Comparing the fluorescence gradient of one skin layer with the fluorescence gradient of a second skin layer, information about the diffusion can be obtained.

DISCUSSION

Variability Within Distribution Profile

The observed variation in the thickness of the stratum corneum and the viable epidermis is due to the local differences within one individual (e.g., desquamating stratum corneum and undulating epidermal-dermal junction) and to the interindividual variations. The obvious deviation in profile of donor 3 compared to donors 1 and 2 is due to pre-selected

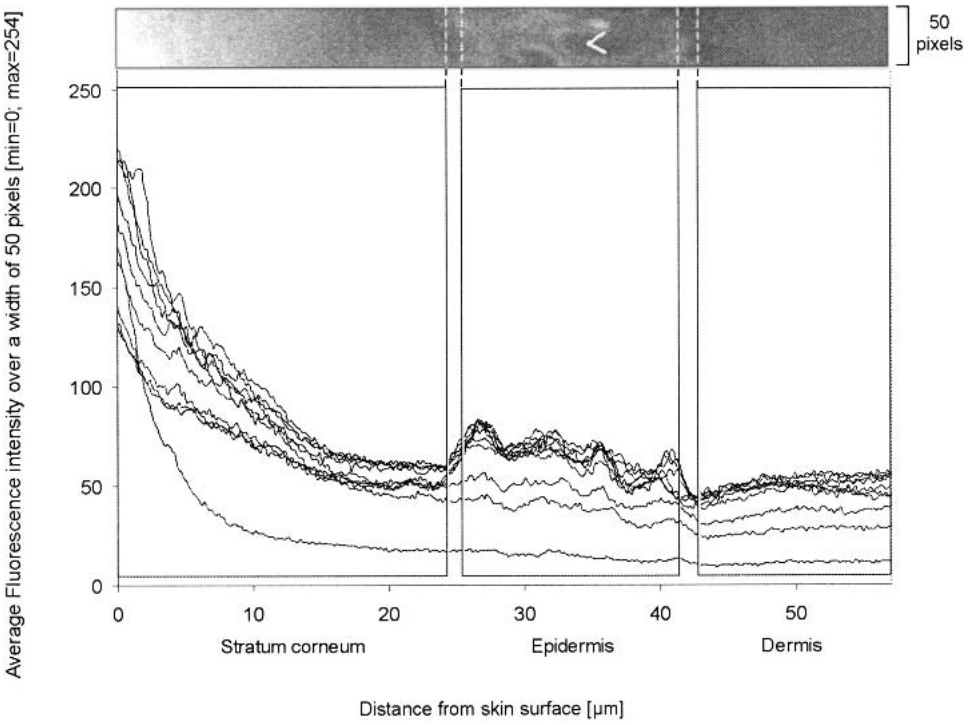

Fig. 4. Distribution profiles of 0.1 mg/ml Bodipy FL C_5 in citric acid buffer pH 5.0 displayed as average fluorescence intensity against depth of one representative donor as detected by confocal laser scanning microscopy. The average intensity was measured by selecting a 50-pixel-wide box (depicted above the donor profile) over the whole thickness of the imaged skin and averaging the value of 50 pixels for every pixel in the depth. Images were recorded every 10 min. To increase clarity of the figure, only distribution profiles of every 40 min are depicted with the lowest line representing 10 min after application. For the complete set of distribution profiles for this donor, see donor 2 of Fig. 5. The area of the respective stratum corneum, epidermis, and first part of the dermis is marked in the graph and as dashed lines in the confocal picture above the graph. Inhomogeneities in the distribution profile of the viable epidermis can be correlated to the nuclei as seen in the confocal image (arrow).

settings of the CLSM. In pilot studies, standard settings for the CLSM were chosen to obtain an adequate signal from the time series as signal optimization cannot be carried out during the diffusion process. When a fluorescence value of 254 is reached, no further increase in fluorescence intensity can be detected although higher fluorescence might be present. Because the intensity in the stratum corneum of donor 3 reaches the maximum after 2 h, no difference with the high value in the epidermis is obtained. The elevated fluorescence of the epidermis however results in a clearer difference of fluorescence intensity between the epidermis and the dermis.

Care should be taken as much as possible to avoid photobleaching, as within one time series this can lead to inconsistencies. One of the reasons for selecting Bodipy FL C_5 is the improved photostability making the dye less sensitive to photobleaching. Bodipy FL C_5 is also reported to be insensitive to solvent polarity and pH (24) and therefore is a suitable model compound for the evaluation of the diffusion pathway. A photobleaching experiment of labeled skin (150 scans) revealed only a minor decrease in fluorescence intensity. Because we did not observe any decrease of fluorescence intensity within time in the experiment, photobleaching is not expected to influence the presented on-line diffusion results.

Distribution Profiles

Although the donor phase was not stirred and exhibited depletion after longer diffusion times and the acceptor phase was static, the obtained curves resemble the ones of the two-layer skin model as reported earlier (25–27). In CLSM, fluorescence intensities of different donors cannot be averaged. Therefore, the fluorescence gradient of Bodipy FL C_5 have been summarized as displayed in Fig. 6. The gradient within the stratum corneum is not constant but varies in depth. The steepest gradient is observed in the upper part of the stratum corneum, where most of the fluorescent label is accumulated. The sudden increase in fluorescence intensity from the dead to the viable epidermis can originate from the absence of cornified envelope and the easy partitioning into the viable epidermis. In the epidermis, the fluorescent intensity gradient is less than in stratum corneum and also varies in depth. The dermis contains fibrous, filamentous, and amorphous connective tissue with a high water-retaining capacity (28), making the dermis rather hydrophilic. The sudden decrease of the fluorescence from the epidermis to the dermis can therefore be explained by the lower affinity of the dermis for a lipophilic substance as Bodipy FL C_5.

Time- and Depth-Resolution

Several studies have been performed to obtain depth profiles of substances within the epidermis and dermis. Caspers *et al.* (14) has obtained a depth profile of Raman active compounds of the skin *in vivo*. Although no diffusion profiles in time have been reported yet, the authors propose

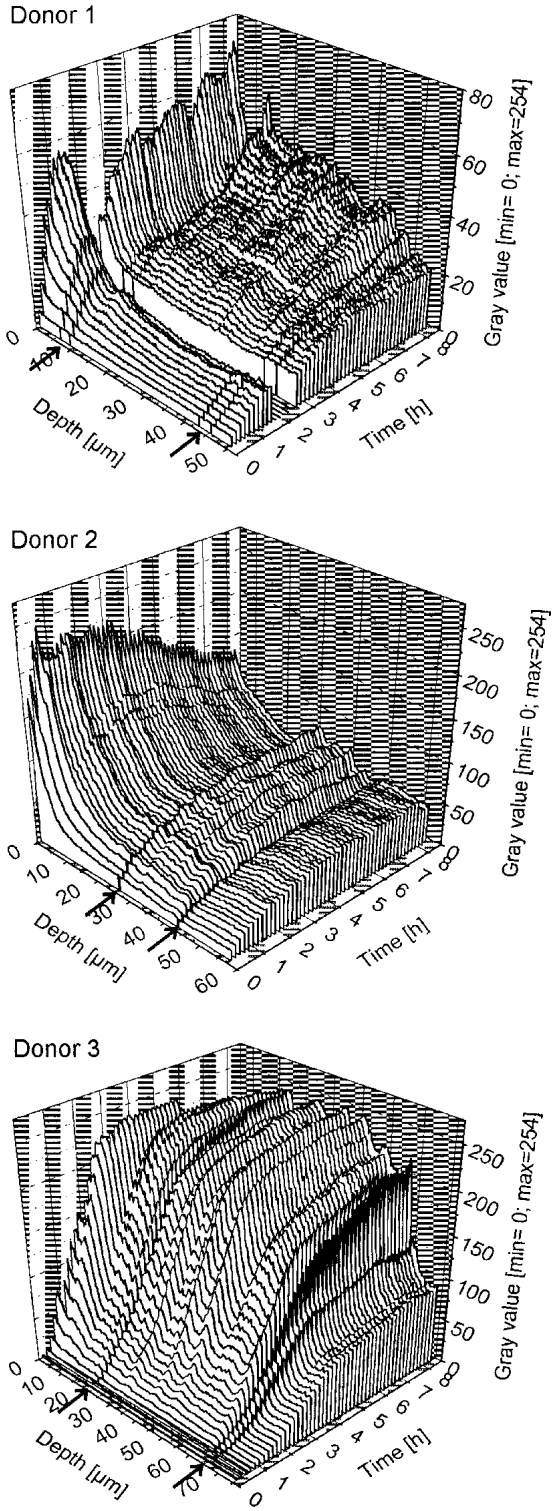

Fig. 5. Three-dimensional distribution profiles of 0.1 mg/ml Bodipy FL C_5 in citric acid buffer, pH 5.0, displayed as average fluorescence intensity against depth and time of three donors as detected by confocal laser scanning microscopy. The average intensity was measured by selecting a 50-pixel-wide box over the whole thickness of the imaged skin and averaging the value of 50 pixels for every pixel in the depth. Images were recorded every 10 min with the lowest line representing 10 min after application. The transition from the stratum corneum to the epidermis and from the epidermis to the first part of the dermis is marked in the graph by arrows.

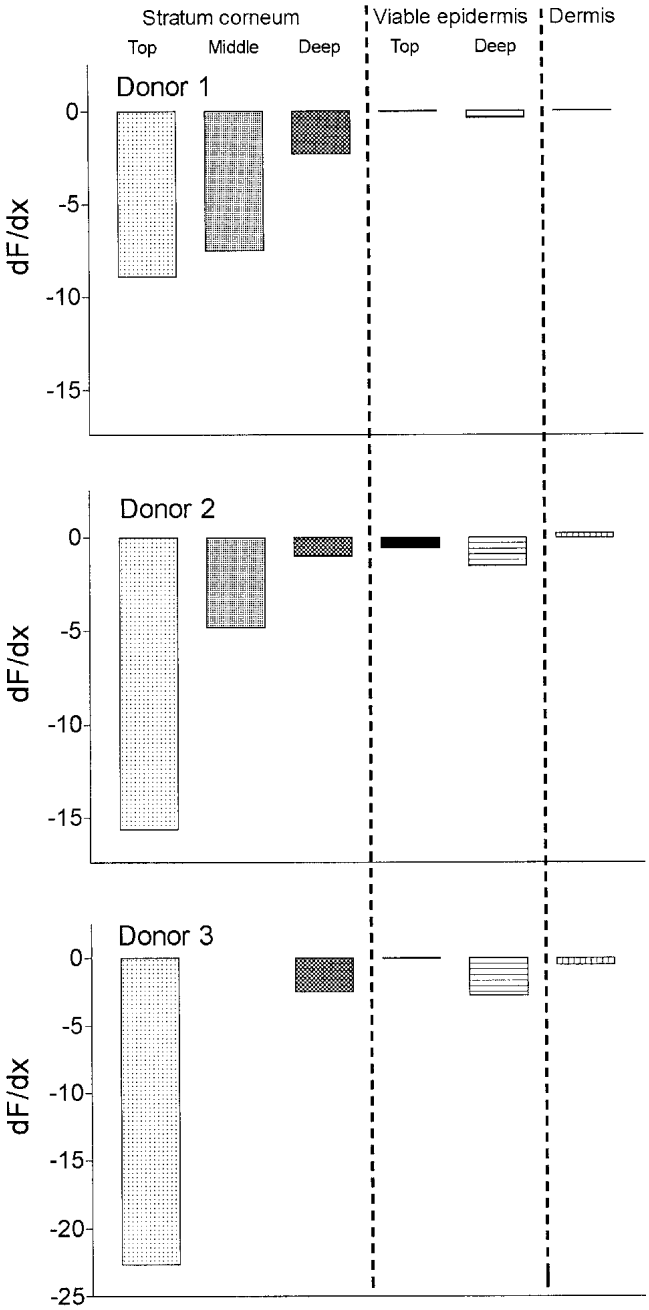

Fig. 6. Fluorescence gradient (dF/dx) in the stratum corneum (top, middle, deep), the viable epidermis (top, deep), and the upper part of the dermis after application of 0.1 mg/ml Bodipy FL C_5 in citric acid buffer, pH 5.0. The fluorescence gradient has been determined from Fig. 5 selecting time points close to steady state. Pre–steady-state diffusion and influences due to dye degradation and donor phase depletion were not included. In donor 3, only two layers of the stratum corneum could be clearly distinguished.

that this technique has the potential to achieve time and depth resolution. Yu *et al.* (29) published distribution profiles of two fluorescent dyes using two-photon CLSM up to a depth of 32 µm. In this case, the on-line diffusion was not studied. Previously, Hoogstraate *et al.* (20) reported concentration gradients of a fluorescent dye in buccal epithelium observed for 2 h. Profiles were measured using narrow boxes parallel to the skin surface. The method presented in this

article extends the method from Hoogstraate *et al.* (20) in three ways. Because in the combined cutting/on-line cell the skin is not moved from the cutting device to the on-line diffusion cell, damage of the freshly obtained cutting surface is prevented. Furthermore, in the current studies only very small variations in the volumes of the acceptor and of the donor phase occur. In the previous studies by Hoogstraate *et al.*, these compartments were created solely by dental clay and varied between the various experiments. Another advantage of this technique is that the measurement of the fluorescence intensity in time is specific per pixel rather than limited to the shape of boxes parallel to the skin surface. Additionally, this new technique has the potential to visualise fluorophores in deeper layers of the skin such as appendages (sweat glands, sebaceous glands, and hair follicles) and the subcutaneous fat.

By estimating the fluorescence gradient for the different skin layers, valuable information can be gained about the diffusion process of substances in intact skin. As mentioned above, the stratum corneum does not reveal a linear fluorescence gradient over the full stratum corneum thickness. It appears that the stratum corneum is not a homogeneous membrane as considered in the various models but that layers at different depths have different diffusion properties. In order to further optimize the experimental setup, a flow-through acceptor and donor phase can be created to rule out depletion and accumulation in any of the phases.

Importantly, the maximum fluorescent gradient in the upper layers of the stratum corneum is formed over a considerate time period. This can be explained as follows. If the deepest layers in the stratum corneum are almost impermeable for the dye, only a limited amount of dye will cross this layer. This will cause, due to its favorable partitioning, an accumulation of the lipophilic dye in the more superficial layers in the stratum corneum, which in turn causes a steep concentration gradient within the stratum corneum. The low fluorescence gradient in the viable epidermis and the fact that the steady-state gradient is reached in a rather short time period proves the absence of a physical barrier function in this layer. Although the lower part of the viable epidermis reveals a higher fluorescence gradient, it is still lower than the fluorescence gradient of the upper 2/3 of the stratum corneum. Once reaching the dermis, the fluorescence gradient is slightly lower implying that the diffusion from the epidermis to the dermis is not rate limiting. Focusing on the partitioning of the lipophilic dye from one skin layer to the adjacent skin layer, it is striking that the partitioning of the dye from the lower stratum corneum to the viable epidermis is high, whereas the partitioning from the epidermis further into the dermis is not favored. This supports the earlier finding of high affinity of the epidermis for this lipophilic label (30,31). Early publications reviewed by Kim *et al.* (32) state that the penetration of highly lipophilic compounds from the epidermis into the dermis can be rate limiting. In case of our lipophilic substance, the rate-limiting step is still within the stratum corneum.

The presented study is the first study in which a fluorescence gradient is measured on-line in fresh and unfixed human skin. Using this method, it is not only possible to measure fluorescent gradients in the main skin layers (stratum corneum, viable epidermis and dermis), but fluorescent intensities can even be distinguished between areas within these layers. However, in this study the fluorescent gradient for the dermis is limited to the first few micrometers and cannot give any information about the deeper layers. Decrease in the magnification would improve the information obtained for the dermal area, but will limit the information on the stratum corneum. In future studies, this technique can be improved by designing a flow-through donor and acceptor phase to create a steady-state situation. Pilot studies performed in our laboratory give indications that a flow-through construction of the donor and acceptor compartment is a feasible modification.

CONCLUSIONS

The presented method enables the visualization and evaluation of time-resolved diffusion into the skin. Fixation and thereby alteration of skin structures and the danger of delocalization of the dye can be circumvented. Due to the cross-sectional view, visualization of structures as far in the skin as the subcutaneous fat can be possible without loss of resolution or sensitivity. Cell structures like nuclei and membranes can be distinguished, which provides the opportunity to observe diffusion processes not only at the skin layer level but as well at the cellular level in the epidermis. This would be of interest to study DNA transfer in cell nuclei. Taking advantage of this time-resolved visualization technique, transport processes can be investigated and delivery systems developed and optimized. In spite of its limitation to fluorophores and *in vitro* studies, the combined cutting device/on-line diffusion cell with CLSM is a promising tool for skin transport studies due to its high resolution, use of non-fixed skin, and access to subcutaneous fat.

ACKNOWLEDGMENTS

We would like to thank Jan Janssen and Henk Verpoorten for the cooperation in the development of the on-line diffusion cell. Furthermore, we acknowledge Unilever Research, Port Sunlight, UK, for financing this project.

REFERENCES

1. P. Corcuff and G. E. Pierard. Skin imaging: State of the art at the dawn of the year 2000. *Skin Bioeng.* **26**:1–11 (1998).
2. E. Touitou, V. M. Meidan, and E. Horwitz. Methods for quantitative determination of drug localized in the skin. *J. Control. Rel.* **56**:7–21 (1998).
3. F. Lund and T. Jogestrand. Video fluorescein imaging of the skin: description of an overviewing technique for functional evaluation of regional cutaneous blood perfusion in occlusive arterial disease of the limbs. *Clin. Physiol.* **17**:619–633 (1997).
4. R. H. Bull, D. O. Bates, and P. S. Mortimer. Intravital videocapillaroscopy for the study of the microcirculation in psoriasis. *Br. J. Dermatol.* **126**:436–445 (1992).
5. J. L. Morris. Cotransmission from sympathetic vasoconstrictor neurons to small cutaneous arteries in vivo. *Am. J. Physiol. Heart Circ. Physiol.* **46**:H58–H64 (1999).
6. T. Salmon, R. A. Walker, and N. K. Pryer. Advances in microscopy-part III; video-enhanced differential interference contrast light microscopy. *Biotechniques* **7**:624–633 (1989).
7. A. W. B. Stanton, H. S. Patel, J. R. Levick, and P. S. Mortimer. Increased dermal lymphatic density in the human leg compared with the forearm. *Microvasc. Res.* **57**:320–328 (1999).
8. S. Richard, B. Querleux, J. Bittoun, I. Idy-Peretti, O. Jolivet, E. Cermakova, and J. L. Leveque. In vivo proton relaxation times analysis of the skin layers by magnetic resonance imaging. *J. Invest. Dermatol.* **97**:120–125 (1991).
9. H. K. Song, F. W. Wehrli, and J. F. Ma. In vivo MR microscopy of the human skin. *Magn. Reson. Med.* **37**:185–191 (1997).
10. M. Szayna and W. Kuhn. In vivo and in vitro investigations of

hydration effects of beauty care products by high-field MRI and NMR microscopy. *Eur. Acad. Dermatol. Venereol.* **11**:122–128 (1998).
11. T. Herrling, J. Fuchs, and N. Groth. Kinetic measurements using EPR imaging with a modulated field gradient. *J. Magn. Reson.* **154**:6–14 (2002).
12. D. H. Turnbull, B. G. Starkoski, K. A. Harasiewicz, J. L. Semple, L. From, A. K. Gupta, D. N. Sauder, and F. S. Foster. 40-100 MHz B-SCAN ultrasound backscatter microscope for skin imaging. *Ultrasound Med. Biol.* **21**:79–88 (1995).
13. P. J. Caspers, G. W. Lucassen, R. Wolthuis, H. A. Bruining, and G. J. Puppels. In vitro and in vivo Raman spectroscopy of human skin. *Biospectroscopy* **4**:S31–S39 (1998).
14. P. J. Caspers, G. W. Lucassen, E. A. Carter, H. A. Bruining, and G. J. Puppels. In vivo confocal Raman microspectroscopy of the skin: noninvasive determination of molecular concentration profiles. *J. Invest. Dermatol.* **116**:434–442 (2001).
15. D. Aghassi, R. R. Anderson, and S. Gonzalez. Time-sequence histologic imaging of laser-treated cherry angiomas with in vivo confocal microscopy. *J. Am. Acad. Dermatol.* **43**:37–41 (2000).
16. C. Bertrand and P. Corcuff. In vivo spatio-temporal visualization of the human skin by real-time confocal microscopy. *Scanning* **16**:150–154 (1994).
17. P. Corcuff, C. Bertrand, and J. L. Leveque. Morphometry of human epidermis in vivo by real-time confocal microscopy. *Arch. Dermatol. Res.* **285**:475–481 (1993).
18. C. Cullander. Light microscopy of living tissue: the state and future of the art. *J. Invest. Dermatol. Symp. Proc.* **3**:166–171 (1998).
19. B. S. Grewal, A. Naik, W. J. Irwin, G. Gooris, G. J. de-Grauw, H. G. Gerritsen, and J. A. Bouwstra. Transdermal macromolecular delivery: Real-time visualization of iontophoretic and chemically enhanced transport using two-photon excitation microscopy. *Pharm. Res.* **17**:788–795 (2000).
20. A. J. Hoogstraate, C. Cullander, J. F. Nagelkerke, F. Spies, J. Verhoef, A. H. G. J. Schrijvers, H. E. Junginger, and H. E. Bodde. A novel in-situ model for continuous observation of transient drug concentration gradients across buccal epithelium at the microscopical level. *J. Control. Rel.* **39**:71–78 (1996).
21. M. Rajadhyaksha, S. Gonzalez, J. M. Zavislan, R. R. Anderson, and R. H. Webb. In vivo confocal scanning laser microscopy of human skin II: advances in instrumentation and comparison with histology. *J. Invest. Dermatol.* **113**:293–303 (1999).
22. M. E. M. J. Meuwissen, J. Janssen, C. Cullander, H. E. Junginger, and J. A. Bouwstra. A cross-section device to improve visualization of fluorescent probe penetration into the skin by confocal laser scanning microscopy. *Pharm. Res.* **15**:352–356 (1998).
23. Y. Y. Grams and J. A. Bouwstra. A new method to determine the distribution of a fluorophore in scalp skin with focus on hair follicles. *Pharm. Res.* **19**:350–354 (2002).
24. J. Karolin, L. B. A. Johansson, L. Strandberg, and T. Ny. Fluorescence and absorption spectroscopic properties of Dipyrrometheneboron difluoride (BODIPY) derivatives in liquids, lipid membranes, and proteins. *J. Am. Chem. Soc.* **116**:7801–7806 (1994).
25. H. Okamoto, F. Yamashita, K. Saito, and M. Hashida. Analysis of drug penetration through the skin by the two-layer skin model. *Pharm. Res.* **6**:931–937 (1989).
26. R. J. Scheuplein and L. W. Ross. Mechanism of percutaneous absorption. V. *J. Invest. Dermatol.* **62**:353–360 (1974).
27. F. Yamashita, H. Bando, Y. Koyama, S. Kitagawa, Y. Takakura, and M. Hashida. In vivo and in vitro analysis of skin penetration enhancement based on a two-layer diffusion model with polar and nonpolar routes in the stratum corneum. *Pharm. Res.* **11**:185–191 (1994).
28. H. Schaefer and T. E. Redelmeier. *Skin Barrier: Principles of Percutaneous Absorption,* Karger, Basel, 1996.
29. B. Yu, C. Y. Dong, P. T. So, D. Blankschtein, and R. Langer. In vitro visualization and quantification of oleic acid induced changes in transdermal transport using two-photon fluorescence microscopy. *J. Invest. Dermatol.* **117**:16–25 (2001).
30. Y. Y. Grams and J. A. Bouwstra. Penetration and distribution of three lipophilic probes in vitro in human skin focusing on the hair follicle. *J. Control. Rel.* **83**:253–262 (2002).
31. Y. Y. Grams, S. Alaruikka, L. Lashley, J. Caussin, L. Whitehead, and J. A. Bouwstra. Permeant lipophilicity and vehicle composition influence accumulation of dyes in hair follicles of human skin. *Eur. J. Pharm. Sci.* **18**:329–336 (2003).
32. Y. H. Kim, A. H. Ghanem, and W. I. Higuchi. Model studies of epidermal permeability. *Semin. Dermatol.* **11**:145–156 (1992).